Journal of Materials Science: Materials in Electronics (2018) 29:9184–9192
https://doi.org/10.1007/s10854-018-8946-y

One-pot synthesis of highly luminescent and color-tunable water-soluble Mn:ZnSe/ZnS core/shell quantum dots by microwave-assisted method

Xiangxin Xue[1] · Lei Chen[1] · Cuimei Zhao[1] · Limin Chang[1]

Received: 12 July 2017 / Accepted: 16 March 2018 / Published online: 24 March 2018

Abstract
In this paper, microwave-assisted method was used for rapid synthesis of highly luminescent Mn-doped ZnSe/ZnS core/shell nanocrystals in aqueous phase. A series of nanocrystals with different size was prepared in 1 h under proper condition. The as-prepared Mn-doped ZnSe/ZnS QDs exhibit the emission in the range of 565–602 nm and the highest photoluminescence quantum yield reached up to 36.3% under the optimal reaction condition. The optical properties and structure of the Mn:ZnSe/ZnS QDs have been characterized by PL spectroscopy, UV–Vis, TEM, XRD and XPS. The effects of various experimental variables, including the reaction pressure, the pH value of reaction solution, the ratio of Zn to ligand (MPA), and the post-treatment on the optical properties of the Mn:ZnSe/ZnS QDs were investigated systematically. The as-prepared MPA coated Mn-doped ZnSe/ZnS colloidal nanoparticles was utilized to ultrasensitively and selectively detect Hg^{2+} ions in water, the result shows that the QD-based metal ions sensor possesses high sensitivity and selectivity, and could be applied for the quantification analysis of Hg^{2+} ions in water.

1 Introduction

Over the past two decades, semiconductor nanocrystals or quantum dots (QDs) have attracted considerable attention due to their potential applications in photoelectric devices and biological imaging and diagnosis, etc [1–6]. So far, cadmium-based semiconductor nanocrystals with highly photoluminescence quantum yield (e.g. CdS, CdSe and CdTe) can be successfully prepared by the organometallic or aqueous methods, and great progress has also been made in controllable synthesis of the core/shell structured QDs that have higher emission efficiency and better photostability compared with the pure cores [7–10]. However, the inherent toxicity of Cd to both the living body and natural environment has made the cadmium-based QDs at a disadvantage in many practical applications [10–14].

In order to suppress the toxicity of Cd-based QDs, scientists have developed many approaches to fabricate lower toxicity of the Cd-based QDs, such as coating the Cd-based QDs with nontoxic ZnS, SiO_2 and polymer shell [15–17]. However, these efforts cannot prevent the leakage of the cadmium and completely eliminate the toxicity of cadmium. Doping of nontoxic Zn-based QDs is considered as a powerful technology to mitigate the toxicity problems. Incorporation of dopant ions can greatly alter the optical and electronic properties of host QDs. Compared with the pure QDs, doped QDs have some special advantages such as longer fluorescence lifetime and higher thermal stability [18–20]. Mn:ZnSe nanocrystals were first successful synthesized using the organometallic hot injection method by Meijerink's group in 2000. In 2005, Peng's group developed so-called nucleation doping and growth-doping strategies for the preparation of Mn:ZnSe d-dots, and using the nucleation doping approach, high photoluminescent Mn:ZnSe nanocrystals were successfully prepared by the organometallic hot injection method [18]. In order to apply semiconductor nanocrystals to the biological system, it is necessary to directly synthesize the nanocrystals in aqueous phase. Compared to organometallic method, aqueous synthesis

Electronic supplementary material The online version of this article (https://doi.org/10.1007/s10854-018-8946-y) contains supplementary material, which is available to authorized users.

✉ Limin Chang
aaaa2139@163.com

[1] Key Laboratory of Preparation and Applications of Environmental Friendly Materials (Jilin Normal University), Ministry of Education, Changchun 130103, China

method has been proved simpler, lower cost, more environmentally friendly and better biocompatibility. In 2009, Wang et al. reported the first case of doped Mn:ZnSe QDs with 3-mercaptopropionic acid (MPA) as the capping reagent in aqueous solution [18]. Later, Aboulaich et al. and Dong et al. reported the preparation of aqueous core/shell Mn:ZnSe/ZnS d-dots with improved photoluminescence efficiency and stability [21, 22].

Compared with conventional aqueous method, the synthesis of nanocrystals by microwave irradiation was generally cheaper, less toxic, faster, simpler, and very energy efficient [23–25]. Some groups have reported about microwave assisted synthesis Mn-doped and Zn-based nanocrystals [26–28]. However, there is little report about a one-pot approach to prepare Mn:ZnSe/ZnS core/shell d-dots in aqueous solution. Meanwhile, the synthesis of Mn:ZnSe/ZnS QDs usually spend a long time (several hours), the as-prepared Mn:ZnSe/ZnS QDs have a low luminescent efficiency (< 30%). In this paper, we report a one-pot synthesis water-soluble Mn:ZnSe/ZnS core/shell QDs by microwave-assisted method using MPA as stabilizer. The experiment results proved that the reaction pressure, the pH value of the reaction solution, the ratio of Zn to MPA and the adsorption of oxygen on the surface have great influence on the optical properties. Under the optimal reaction condition, a series of Mn:ZnSe/ZnS d-dots was prepared in 1 h, the as-prepared QDs exhibit emission in the range of 565–602 nm and highly photoluminescence quantum yield reached up to 36.3%.

2 Experiment

2.1 Chemicals

Analytical grade $Zn(Ac)_2{\cdot}2H_2O$ and sodium borohydride were obtained from Sigma-Aldrich, 3-mercaptopropionic acid (MPA) was a product of Fluka, Rhodamine 6G was purchased from Sigma-Aldrich, and selenilum metal powder was purchased from Shanghai Meixin. $Hg(NO_3)_2{\cdot}H_2O$, $CoCl_2{\cdot}6H_2O$, $AgNO_3$, $Ni(NO_3)_2{\cdot}6H_2O$, $CuSO_4{\cdot}5H_2O$, $CdCl_2{\cdot}2.5H_2O$, $Pb(NO_3)_2$, $FeCl_3{\cdot}6H_2O$, $CrCl_3{\cdot}6H_2O$, $MgCl_2{\cdot}6H_2O$, $ZnCl_2$ were purchased from Tianjin Recovery Fine Chemical Industry Research Institute (Tianjin, China). All the reagents were at least of analytical grade and were used as received without further purification. High-purity water (Pall Purelab Plus) with a resistivity of 18.2 MΩ cm^{-1} was used for the preparation of all aqueous solution.

2.2 Synthesis of Mn:ZnSe/ZnS QDs by microwave irradiation

A microwave digestion system (MDS-2003F) made by Shanghai SINEO Instruments was used for the preparation of Mn-doped ZnSe/ZnS core/shell QDs, which was equipped with controllable pressure units. The system can operate at 0–4 MPa and work at 0–1000 W power. The reaction temperature and time can be programmed by users. The synthesis of nanocrystals was performed in lined digestion vessels that are double-walled vessels consisting of a Teflon inner liner and cover surrounded by a high-strength vessel shell of Ultem polyetherimide. The volume of vessel used in the reaction was 60 mL. In general, the monomers solution occupied 1/6 volume of the vessel, and air filled the rest of the space. In a typical experiment, 0.2240 g $Zn(Ac)_2$ $2H_2O$ (1 mmol) was diluted to 90 mL with water, 3 mL of 0.01 M $Mn(Ac)_2$ and different volume of MPA were mixed together, the pH of the mixed solution was adjusted with 1 M NaOH (7.3–12.3). After the purging of air by N_2 bubbling for 15 min, sodium hydroselenide (prepared by mixing sodium borohydride and selenium powder in oxygen free water) was quickly injected into the solution. The molar ratio of Zn^{2+}:NaHSe is 4:1, the MPA/Zn ratio was varied from 4 to 8. Then Mn-doped ZnSe/ZnS core/shell QDs grew at microwave irradiation (0.6–1.0 MPa, 400 W). All the experiments were repeated three times.

2.3 Detection of mercury ion

5 mL different concentrations of mercury ion solution (0–20 nM) were prepared for further use. Different concentration Hg^{2+} ion solution was added into 1 mL of the as-prepared colloidal nanoparticles solution. After incubating for 30 s (by means of several measurements, 30 s as a response time is enough to obtain stable fluorescent data), the fluorescence emission spectra were measured at excitation wavelength of 400 nm, each spectrum was collected repeatedly for at least three times. Therefore, PL intensity of probe solution at 582 nm as a function of time was measured after adding mercury ions. Experimental conditions for other ten heavy metal ions were the same as those for Hg^{2+} ions (20 nM).

2.4 Sample characterization

X-ray diffraction (XRD) patterns were collected on a Rigaku D/max XRD with Cu KR radiation (λ = 1.5405 Å). The surface morphology of the samples was measured on a Hitachi H-8100 transmission electron microscope (TEM) operated at an acceleration voltage of 200 kV. X-ray photoelectron spectra (XPS) were investigated by using an Escalab 250 Xi spectrometer. Fluorescence spectra of nanocrystal samples in aqueous solution were obtained at room temperature with a FS900 steady-state fluorescence spectrometer with a 450 W xenon lamp as excitation source. UV–Vis measurements were performed on a Varian Cary-100 spectrometer.

The fluorescence QY of nanocrystals was determined from the integrated fluorescence intensities of the nanocrystals and the reference (Rhodamine 6G solution in ethanol, QY = 94.5% at 350 nm excitation).

$$QYs = (Fs \times Ar \times QYr)/(Fr \times As) \quad (1)$$

where Fs and Fr are the integrated fluorescence emissions of the sample and the reference, respectively; As and Ar are the absorbance at the excitation wavelength of the sample and the reference, respectively; QYs and QYr are the quantum yields of the sample and the reference, respectively.

3 Results and discussion

3.1 Results of Mn^{2+}-doped ZnSe/ZnS core/shell quantum dots

Under optimal experiment condition, a series of Mn:ZnSe/ZnS core/shell nanocrystals with different photoluminescence color were synthesized in 1 h by microwave-assistant methods. Figure 1a, b show the PL and UV–Vis spectra of the as-prepared Mn:ZnSe/ZnS core/shell nanocrystals, both the PL and absorbance peaks gradually red shift with the increasing of sizes, the absorbance edge change from 410 to 450 nm, the as-prepared QDs exhibits emission in the range of 565–602 nm, the image shows the tunable luminescence color from yellow–green, orange to red, and the highest photoluminescence quantum yield can reach up to 36.3%. To understand the crystal structure of the as-prepared Mn:ZnSe/ZnS QDs, the wide-angle XRD patterns were collected (Fig. 2). The three main peaks correspond to the (111), (220) and (311) planes (JCPDS Card No. 80-0021), respectively, showing that the as-prepared samples have a cubic zinc blend structure. Meanwhile, the diffraction peaks locate in between ZnSe (bottom) and ZnS (top), and gradually shift to wide angle region approached those of ZnS crystals, which is attributed to the ZnS shell formation and the shell thickness gradually increasing.

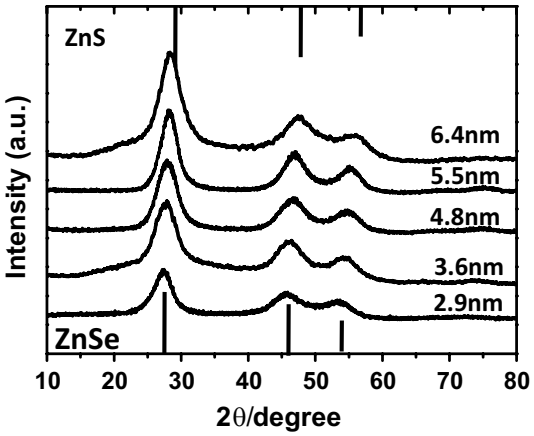

Fig. 2 XRD pattern of representative Mn-doped ZnSe/ZnS core/shell nanocrystals

TEM measurement was performed to understand the morphology of the Mn:ZnSe/ZnS QDs (Fig. 3). The TEM result shows that the as-prepared Mn:ZnSe/ZnS QDs are highly monodispered and homogeneous, and the size of the three representative samples are 3.6 nm (a), 4.8 nm (b) and 6.4 nm (c), respectively, which are consistent with the XRD results calculated by the Scherrer equation. Meanwhile, the as-prepared QDs has good crystallinity as the HTEM image shown in Fig. 3d.

The different experiment condition have great influence on the optical properties of color-tunable Mn-doped ZnSe/ZnS core/shell nanocrystals, to obtain high quality QDs, we systematically investigated the influence of different experimental parameters, including the reaction pressure, the pH value, the molar ratio of Zn to MPA, and the adsorption of oxygen on the surface of QDs.

3.2 The influence of microwave irradiation

The microwave irradiation plays an important role in one-pot aqueous synthesing Mn-doped ZnSe/ZnS core/shell nanocrystals because it can provide higher reaction

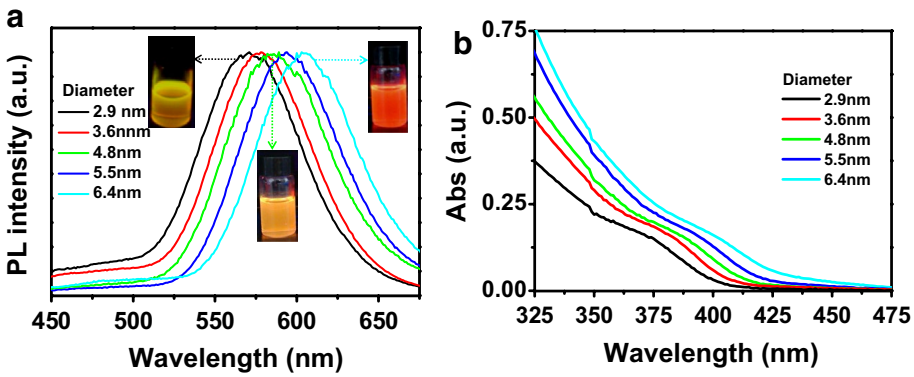

Fig. 1 The photoluminescence (**a**) and absorbance spectra (**b**) of as-prepared Mn:ZnSe/ZnS QDs with different size

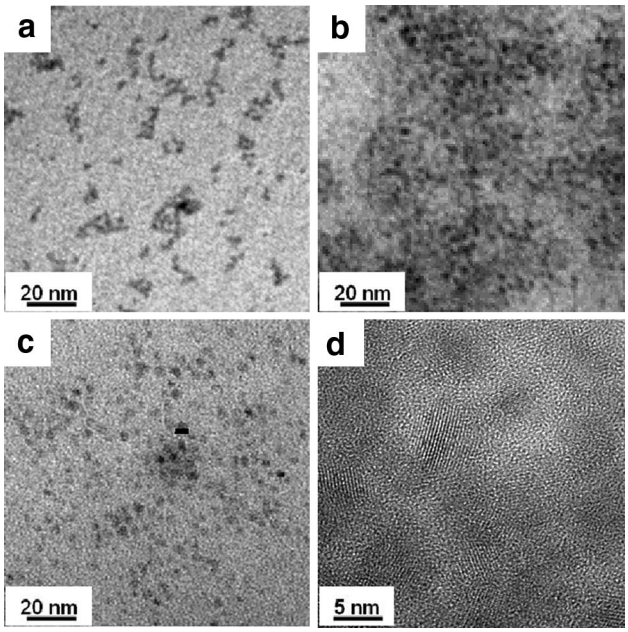

Fig. 3 TEM (**a**–**c**) and HTEM (**d**) images of representative Mn-doped ZnSe/ZnS core/shell nanocrystals

temperature and pressure. It is difficult to prepare high quality Mn-doped ZnSe/ZnS core/shell nanocrystals by using conventional aqueous method, the experiment results were shown in Fig. 4. The samples show stronger trapped emission between 400 and 500 nm and without Mn-doped center-related emission in the beginning several hour. After heating for 5 h, the weakly Mn-doped center-related emission (565 nm) appeared and the PLQY is very low about 0.2%. The absorbance edge shows no obviously shift after heating 3 h, which illuminates the size of the particles does not increase with increasing the heating time. The XRD result (Fig. S1) shows that the as-prepared QDs was Mn-doped ZnSe nanocrystals rather than Mn-doped ZnSe/ZnS core/shell nanocrystals due to the diffraction peaks are consistent with that of ZnSe nanocrystals.

Firstly, we study the effect of the microwave irradiation pressure on the experiment results. Figure 5a shows that the pressure of microwave irradiation (0.6, 0.8 and 1.0 MPa) have effects on the optical properties of Mn:ZnSe/ZnS QDs. The Mn:ZnSe/ZnS QDs was prepared under the same experiment condition except for the pressure of microwave irradiation. But the optical properties show great difference, the PL spectra red shift gradually with the increasing of the microwave irradiation pressure. When the pressure is 0.6 Mpa, the sample shows stronger trapped emission between 400 and 500 nm besides the Mn-doped center-related emission (565 nm). The as-prepared samples exhibit the maximum PL signal at 0.8 Mpa and PL peak locate at 575 nm, its PL spectra includes weak defects emission and strong intrinsic emission. When the pressure is 1.0 Mpa, the PL spectra of

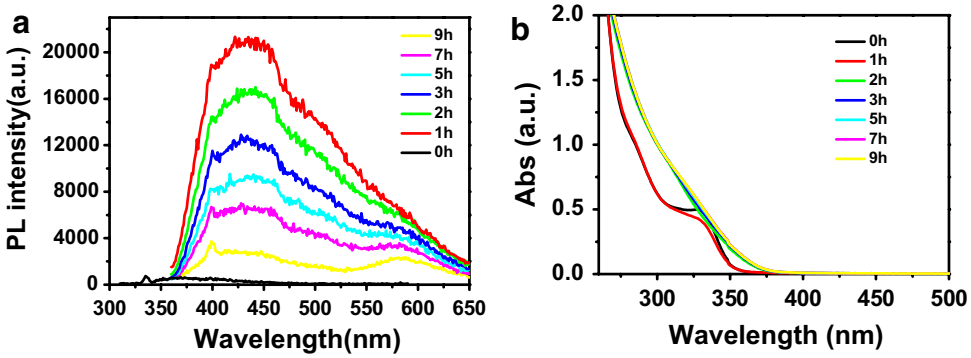

Fig. 4 PL and absorbance spectra of Mn-doped ZnSe nanocrystals prepared under 100 °C oil bath

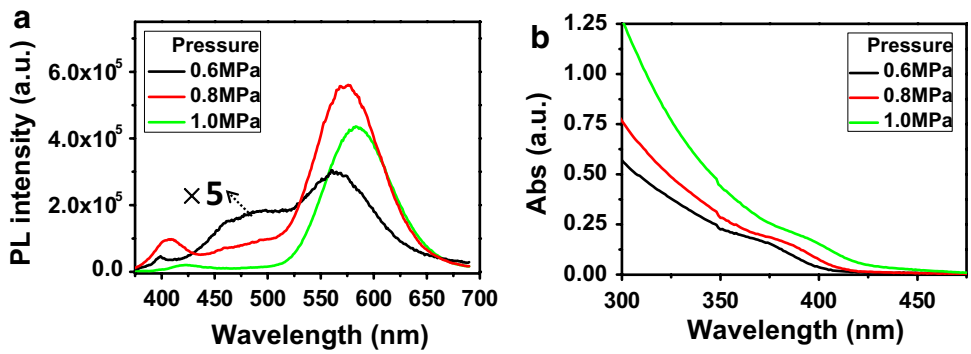

Fig. 5 PL (**a**) and UV–Vis (**b**) spectra of Mn:ZnSe/ZnS QDs at different reaction pressure

Mn:ZnSe/ZnS QDs only shows the Mn-related emission without the defect emission. Meanwhile, the UV–Vis spectra of the Mn:ZnSe/ZnS QDs do not show any observable features at visible wavelengths up to the UV region (350 nm) in accordance with the previous study (Fig. 5b), the absorbance edges of the samples also gradually red shift with enhancing the pressure, which illuminates the formation of ZnS shell on the un-doped partial of ZnSe host. There is a possibility that, the MPA ligands can decompose and release S^{2-} ions as increasing the pressure, and the formation of ZnS shell can passivate the surface defects of ZnSe hosts, so the surface defects related-emission gradually decreased (from 0.6 to 1.0 Mpa). However, when the reaction pressure is too high, the more S^{2-} releasing from MPA can produce S^{2-} related defects on the surface of ZnS shell, which lead to the decrease of Mn-related emission (1.0 Mpa) [26–28]. Therefore, we can conclude that 0.8 Mpa is an appropriate reaction pressure, and we choose the pressure of microwave irradiation of 0.8 Mpa as the reaction pressure in the following experiments.

3.3 The effect of pH value

The pH value of the reaction solution has great influence on the optical properties of the Mn:ZnSe/ZnS QDs. Figure 6a, b show the optical spectra of Mn:ZnSe/ZnS QDs prepared under different pH value from 7.3 to 12.3. We found that the position of the emission peaks, the PL intensity of Mn-related and defects related-emission and the absorbance band edge all have great difference when increasing the pH value. The position of emission peaks gradually shift from 570 to 592 nm as the pH value changing from 7.3 to 12.3 (Fig. 6a, c), the absorbance band edge also gradually red shift from 425 to 450 nm, which illustrate the size of QDs gradually increase and the formation of ZnS shell as the increasing pH value, the absorbance band edge have a great lift at pH = 12.3 because of the strong scattering form the reaction suspension (Fig. 6b). As shown in Fig. 6a, c, the PL intensity of Mn-related and defects related-emission dramatically enhance to the highest value at pH = 9.3, and then reduce to negligible at pH = 12.3. Based on the literatures, we suspected that the effect of pH value on optical properties mainly originate from two aspects. Firstly, the OH^- can compete Mn^{2+} and Zn^{2+} with MPA, and activate Mn and Zn ions to form MnSe and ZnSe, and the optimized parameter is 9.3, since sufficient OH^- ions did not only lead to rapidly form small-sized MnSe cores, which was critically important to improve the PLQY, but also make the ZnSe on the surface of the MnSe diffused core, preventing the oxidation of Mn ions. When pH values increased further, the PL intensity decreased, we believed that a large excess of OH^- ions may cause the formation of the manganese oxide or manganese hydroxide or zinc oxide, which were a disastrous influence on PLQY [29]. Secondly, the pH value influences on the decomposition rate of MPA ligands, and then affect the formation of ZnS shell. The scheme of decomposition of MPA was shown in

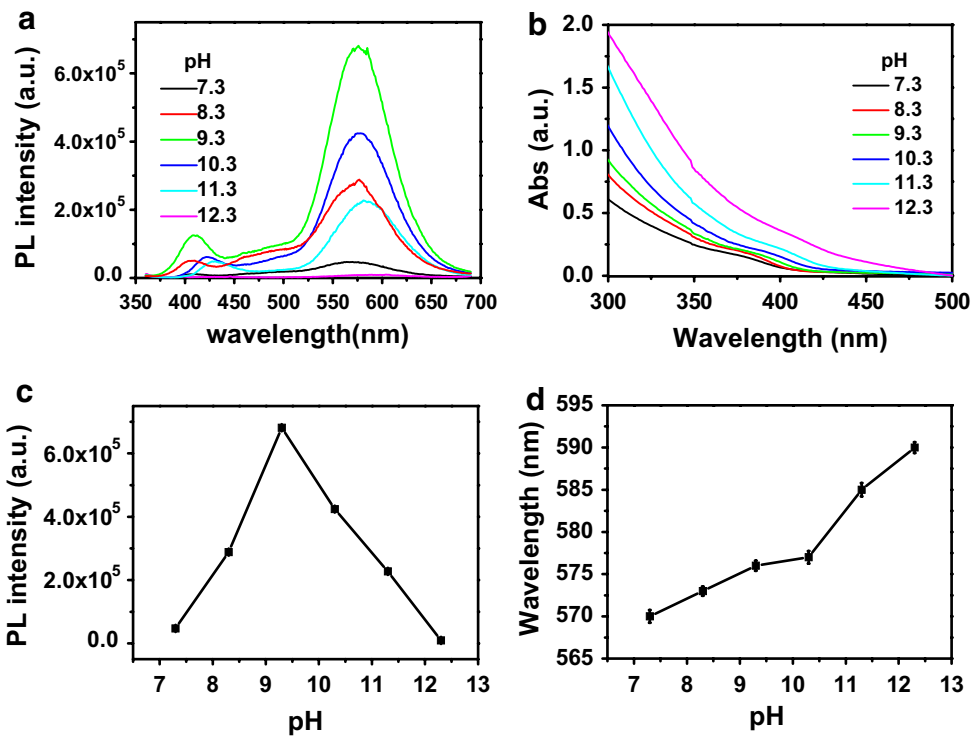

Fig. 6 PL (**a**) and UV–Vis (**b**) spectra of Mn:ZnSe/ZnS QDs preparing at different pH values of MPA precursors, the PL intensity (**c**) and peaks (**d**) change as the pH values

Scheme 1 (Supporting information). At the low pH value, the decomposition of MPA is relatively difficult, which is bad for the formation of ZnS shell, so the as-prepared Mn:ZnSe/ZnS QDs have strong defected-related emission and weak Mn-related emission. As the increasing of pH value, the decomposition of MPA become easier, which is good for the formation of ZnS shell, so the surface defects can be effectively eliminated, the defected-related emission dramatically reduce and the Mn-related emission become stronger. At higher pH value, the decomposition of MPA release too much S^{2-} ions and thus produce the S-related defects on the surface of ZnS shell, which leads to the decrease of Mn-related emission. Meanwhile, there is the possibility of the formation of Zinc Oxide at higher pH value because the OH^- ions can also react with Zn^{2+} at the same time, the formation of white suspension with strong scattering at pH = 12.3 proved this point of view [30]. The XRD data can prove the above point as shown in Fig. S1, all the as-prepared Mn-doped ZnSe/ZnS nanocrystals under different pH have the same zinc blende structure. For the samples prepared at different pH values, the diffraction peaks gradually shifted to wide angle region, approach gradually to those of ZnS crystals. The XRD results mean that the thickness of the ZnS shell gradually increase as the increasing pH value, which illustrate the MPA can easier decompose at higher pH value. The samples prepared at pH = 9.3 have the highest PL intensity, so we will choose pH = 9.3 as the reaction pH value in the next experiment.

3.4 The influence of the ratio of MPA/Zn

The formation of ZnS shell have great effect on the optical properties of Mn:ZnSe/ZnS QDs, it is necessary to study the effect of amount of sulfur source MPA on the optical properties, so we investigate the influence of Zn/MPA ratio on the PL property of the prepared Mn:ZnSe/ZnS QDs. Figure 7a shows the PL spectra of the as-prepared samples under the same reaction conditions beside the Zn/MPA ratio. The Mn-related PL intensity of the prepared Mn:ZnSe/ZnS QDs firstly increased and then decreased with the MPA concentration increasing, and when the ratio of Zn to MPA is 1:5, the PL intensity reached the maximum. The continuous decrease of the ratio of Zn to MPA will cause the decrease of the Mn-related PL intensity, but the defect-related emission gradually weakened to disappear. Meanwhile, the PL peaks red shift from 576 to 595 nm, and the absorbance band edge of all samples also show obviously red shift (Fig. 7b). This is due to the large amount S^{2-} released from MPA will be good for forming ZnS shell, which have great influence on the PL properties. We know that as the increasing of MPA amount, the large amount of S^{2-} released from MPA are good for the formation of ZnS shell, so the surface defects can be effectively eliminated, the defected-related emission dramatically reduce and the Mn-related emission become stronger, when the ratio of MPA to Zn is five shows the maximum luminous efficiency. At higher MPA concentration, the decomposition of excessive MPA release too much S^{2-} ions and thus produce the S-related defects on the surface of ZnS shell, which leads to the decrease of Mn-related emission. The XPS data

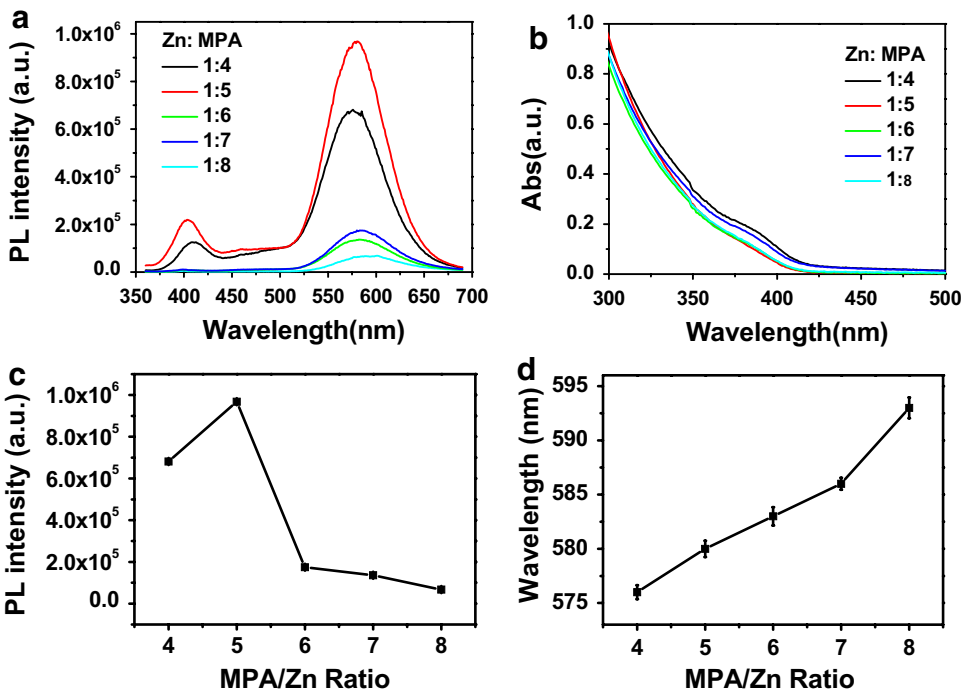

Fig. 7 PL (**a**) and UV–Vis (**b**) spectra of Mn:ZnSe/ZnS QDs preparing at different Zn/MPA ratio, the PL intensity (**c**) and peaks (**d**) change as MPA/Zn ratio

Table 1 Surface atom ratio of Se/Zn and S/Se revealed by XPS analyses of the MPA-capped Mn-doped ZnSe nanocrystals prepared under different Zn/MPA ratio

	Zn/MPA ratio				
	1/4	1/5	1/6	1/7	1/8
Se/Zn	0.42	0.37	0.33	0.28	0.25
S/Se	1.36	1.72	2.04	2.53	2.97

prove the above conclusion. Table 1 shows the XPS analyses were employed to investigate the surface composition of the nanocrystals prepared under different Zn/MPA ratio. Three elements, Zn, Se and S, were observable in all the ZnSe samples investigated (see Supporting information Fig. S2). Contents of the elements were quantified based on the integration areas of the peaks as shown in Table 1. The Se/Zn ratio in the as-prepared samples decreased from 0.42 to 0.25 as the Zn/MPA ratio decreased from 1/4 to 1/8. It is noted that the S/Se ratio was 1.36 for the Mn-doped ZnSe samples prepared at Zn/MPA = 1/4, which increased to 2.97 for the samples prepared at Zn/MPA of 1/8. It is obvious that there is lots of S element on the surface of the Mn-dope ZnSe nanocrystals prepared at excessive MPA ligands. It is supposed that ZnS shell was formed on the surface of the Mn-doped ZnSe nanocrystals, which eliminated the surface defects and thus improved the PLQY of the Mn-doped ZnSe nanocrystals. However, too much S^{2-} ions can produce S-related defect, and thus lead to the decrease of Mn-ralated emission. A typical PL and absorbance spectra Mn:ZnSe/ZnS QDs prepared at pH = 10.3 and Zn:MPA = 1:6 were shown in Figure S4, both of the PL and absorbance spectra gradually shift to long wavelength region as the increasing of ZnS shell growth.

3.5 The influence of adsorbed oxygen

Besides the effect of above factors on the optical properties of Mn-doped ZnSe/ZnS QDs, we find an interesting experiment results that the PL quantum yield of as-prepared Mn-doped ZnSe/ZnS nanocrystals is dramatic improved after aging samples some time (keeping samples in air for some time). With the increase of aging time, the luminescence intensity of quantum dots increases, which indicates that in order to obtain quantum dots with better luminescence intensity, the aging time should be increased as much as possible [31–34]. Figure 8 shows the PLQY change of samples preparing under different pH value, the PLQY of fresh samples (under pH 7.3, 8.3, 9.3, 10.3, 11.3, 12.3) are 3.1, 7.9, 15.2, 9.3, 4.3 and 0.42, respectively. After aging 2 weeks, PLQY of all samples (4.5, 12.3, 36.3, 30.1, 22.6 and 1.8) are improved and up to maximum after 2 weeks. The typical PL spectra of Mn:ZnSe/ZnS QDs prepared at pH 9.3 and

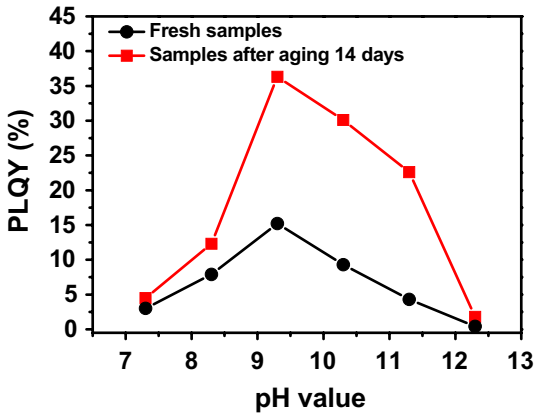

Fig. 8 PLQY of the samples prepared under different pH value before and after aging two weeks

11.3 before and after aging 2 weeks are shown in Fig. 9, the positions of PL peaks are both no obviously changed, but the PL intensity are dramatically enhanced, the inset PL images obtained under 365 nm UV lamp irradiation show that the samples after aging become more bright. Previously studies prove that the dissolved oxygen tend to be absorbed on the surface of ZnS nanocrystals, especially on the surface defect sites [35]. As we all known, the surface defects play an important role in the optical properties of nanocrystals, when there is oxygen in the freshly samples solution, the dissolved oxygen tends to be absorbed on activated surface defect sites, and thus the surface defects will be blocked efficiently, the nonradiative recombination will be suppressed because of the formation of oxide species, thus the luminescence of the Mn-doped ZnSe/ZnS nanocrystals are greatly improved [29].

In summary, the pressure of the microwave irradiation, the pH values of the reaction solution and the ratio of Zn to MPA ligands have effect on the S^{2-} release from the decomposition of MPA and form ZnS shell on the surface of Mn-doped ZnSe QDs, which are very important for the optical properties of as-prepared Mn-doped ZnSe/ZnS core/shell nanocrystals. Meanwhile, the oxygen in air may dissolve into the samples solution during the aging time, and will eliminate lots of surface defects, and it is good for improving PL efficiency.

3.6 Application in selective detection of mercury in water

Mercury ions are one of the highly toxic heavy metal ions and environmental pollutants, extensively exist in a variety of water systems, and easily cause great permanent damage to human health and ecological environment even at a trace amount. Therefore, ultrasensitive detection of mercury is essential to provide evaluation criteria of mercury ions in

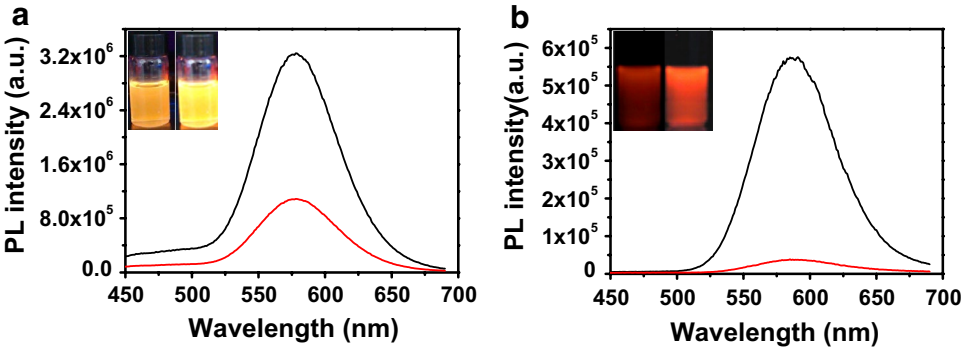

Fig. 9 PL spectra of Mn:ZnSe/ZnS QDs after aging two weeks, **a** pH = 9.3 and **b** pH = 11.3. The inset pictures are PL photos under 365 nm UV lamp before and after aging

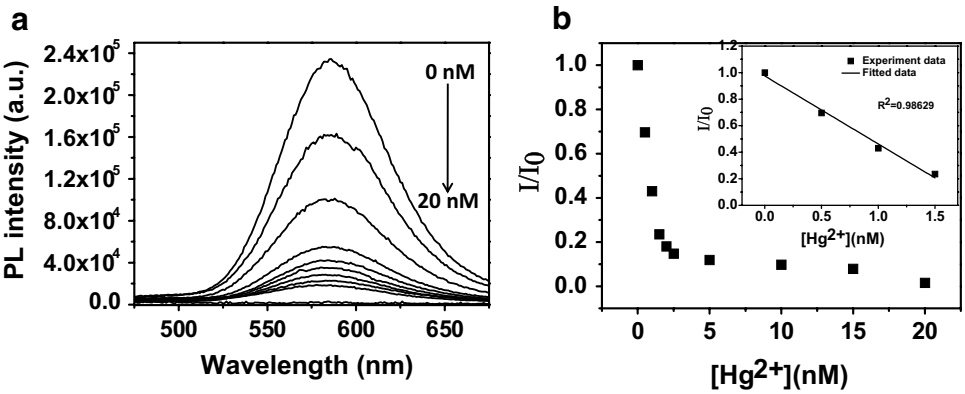

Fig. 10 **a** Photoluminescence spectra of the Mn-doped ZnSe/ZnS QDs in PBS buffer (pH = 7.4) in the presence of different concentrations of Hg^{2+} ions (0–20 nM). **b** Calibration curve of the QD fluorescence at 582 nm vs. [Hg^{2+}] (0–1.5 nM). The inset: a linear relationship between I/I_0 at 582 nm vs. [Hg^{2+}] (0–1.5 nM), $R^2 = 0.98629$

aqueous environment [36]. In this study, the as-prepared water-soluble Mn-doped ZnSe/ZnS QDs were successfully applied to detect Hg^{2+} in water samples with advantages of simplicity, rapidity, sensitivity, and high selectivity. Adding different concentrations of Hg^{2+} ions into water-soluble Mn-doped ZnSe/ZnS colloidal nanoparticles, we can observe the obviously change of the photoluminescence spectra (Fig. 10), which shows the fluorescence intensity of MPA-coated QDs in the presence of Hg^{2+} ions (0–20 nM) in the PBS (5 mM, pH = 7.4) buffer solution. The emission intensity of QDs was quenched obviously with the addition of Hg^{2+}. Meanwhile, the clear solution rapidly became turbid due to the aggregation of colloidal nanoparticles. The aggregation of colloidal nanoparticles is attributed to the separation of the ligands layer from the surface of colloidal nanoparticles in the presence of Hg^{2+} ions because of the strong interaction between thiol(s) and mercury ions. The emission signal response to mercury ions could thus be utilized to detect mercury ions in aqueous solution. The limit of detection (LOD) of the as-prepared Mn-doped ZnSe/ZnS chemosensor is 0.1 nM which is lower than those of QDs chemosensors reported by other research groups. Based on the data obtained using the above procedure, the linear range from 0 to 1.5 nM was linear fitted into the equation of $I/I_0 = 0.9744 - 0.5122 \times C$, where C is the concentration of Hg^{2+} ions in samples (Fig. 10b inset).

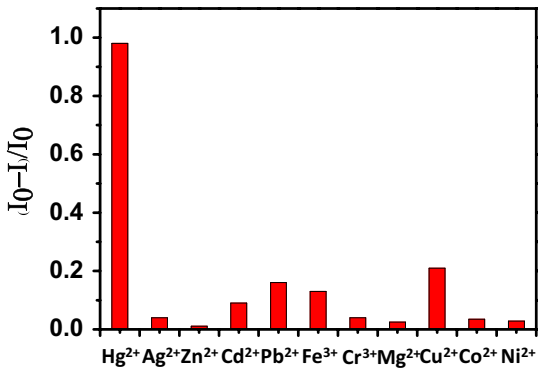

Fig. 11 The fluorescent response of the Mn-doped ZnSe/ZnS QDs ($\lambda_{max} = 582$ nm) in the presence of various heavy metal ions at 20 nM. The excitation wavelength was 400 nm

In order to investigate the selective interaction between colloidal nanoparticles and Hg^{2+} which is necessary for practical applications, the luminescence spectra of colloidal nanoparticles were collected in the presence of other ten heavy metal ions besides Hg^{2+}, including Ag^{+}, Zn^{2+}, Cd^{2+}, Pb^{2+}, Fe^{3+}, Cr^{3+}, Mg^{2+}, Cu^{2+}, $Co^{2+}$and Ni^{2+}. MPA-coated Mn-doped ZnSe/ZnS QDs did not show large responses to these metal ions (Fig. 11). The experiment result illustrates that these heavy metal ions only slightly quenched

the photoluminescence of QDs due to the weak interaction between the thiol functional group and these heavy metal ions. The as-prepared Mn-doped ZnSe/ZnS chemosensor shows a high sensitivity and selectivity to mercury ions, which indicates that it can be applied to the detection of mercury ions in water.

4 Conclusion

In this work, water-soluble Mn-doped ZnSe/ZnS core/shell QDs with MPA as stabilizer was fabricated by a rapid microwave method. It was found that the optical properties of the Mn:ZnSe/ZnS QDs can be affected by the reaction pressure, the pH value of reaction solution, the ratio of Zn to ligand (MPA), and the adsorption of oxygen on the surface. By rationally changing the factors above, a series of highly luminescent and color tunable Mn:ZnSe/ZnS core/shell QDs were prepared with the highest PLQY ~ 36.3%, the as-prepared high luminescent doped QDs have also been successfully used for ultrasensitively and selectively detection of Hg^{2+} ions in water, and this work will be helpful for the aqueous preparation of doped nanocrystals with high luminescent.

Acknowledgements This study was financially supported by the National Natural Science Foundation (Grant Nos. 21505049) of P. R. China; the Development Program of Science and Technology of Jilin Province (20170520134JH); the Scientific Foundation for Young Scientists of Jilin Normal University (2014005 and 2014007).

References

1. B.J. Marcel, M. Mario, G. Peter, W. Shimon, A.P. Alivisatos, Science **281**, 2013 (1998)
2. W.C.W. Chan, S.M. Nie, Science **281**, 2016 (1998)
3. M. Han, X. Gao, J.Z. Su, S.M. Nie, Nat. Biotechnol. **19**, 631 (2001)
4. I.L. Medintz, H.T. Uyeda, E.R. Goldman, H. Mattoussi, Nat. Mater. **4**, 435 (2005)
5. J. Weng, J. Ren, Curr. Med. Chem. **13**, 897 (2006)
6. Q.J. Sun, Y.A. Wang, L.S. Li, D.Y. Wang, T. Zhu, J. Xu, C.H. Yang, Y.F. Li, Nat. Photonics **1**, 717 (2007)
7. N. Pradhan, X. Peng, J. Am. Chem. Soc. **129**, 3339 (2007)
8. H.Z. Wang, H. Nakamura, M. Uehara, Y. Yamaguchi, M. Miyazaki, H. Maeda, Adv. Funct. Mater. **15**, 603 (2005)
9. H.Z. Wang, H.Y. Li, M. Uehara, Y. Yamaguchi, H. Nakamura, M. Miyazaki, H. Shimizu, H. Maeda, Chem. Commun. **1**, 48 (2004)
10. M. Green, E. Howman, Chem. Commun. **7**, 121 (2005)
11. R. Bakalova, Z. Zhelev, H. Ohba, Y. Baba, J. Am. Chem. Soc. **127**, 9328 (2005)
12. Y.C. Wang, B. Wu, C.B. Yang, M.X. Liu, T.C. Sum, K.T. Yong, Small **12**, 534 (2016)
13. J. Heo, C.S. Hwang, Nanomaterials **6**, 82 (2016)
14. M. Anilkumar, K.R. Bindu, A.S. Saj, E.I. Anila, Chinese Phys. B **25**, 088103 (2016)
15. T. Kezuka, M. Konishi, T. Isobe, M. Senna, J. Lumin. **418**, 87 (2000)
16. L. Cao, J. Zhang, S. Ren, S. Huang, Appl. Phys. Lett. **80**, 4300 (2002)
17. S. Ethiraj, N. Hebalkar, S.K. Kulkarni, R. Pasricha, J. Urban, C. Dem, M. Schmitt, W. Kiefer, L. Weinhardt, S. Joshi, R. Fink, C. Heske, E. Umbach, J. Chem. Phys. **118**, 8945 (2003)
18. N. Pradhan, D. Goorskey, J. Thessing, X. Peng, J. Am. Chem. Soc. **127**, 17586 (2005)
19. N. Pradhan, D.M. Battaglia, Y. Liu, X. Peng, Nano Lett. **7**, 312 (2007)
20. D.J. Norris, A.L. Efros, S.C. Erwin, Science **319**, 1776 (2008)
21. A. Aboulaich, M. Geszke, L. Balan, J. Ghanbaja, G. Medjahdi, R. Schneider, Inorg. Chem. **49**, 10940 (2010)
22. B.H. Dong, L.X. Cao, G. Su, W. Liu, J. Phys. Chem. C **116**, 12258 (2012)
23. H.F. Qian, X. Qiu, L. Liang, J.C. Ren, J. Phys. Chem. B **110**, 9034 (2006)
24. M.A. Correa-Duarte, M. Giersig, N.A. Kotov, L.M. Liz-Marzan, Langmuir **14**, 6430 (1998)
25. L. Li, H.F. Qian, J.C. Ren, Chem. Commun. **36**, 528 (2005)
26. D.M. Han, C.F. Song, X.Y. Li, Spectrosc Spect Anal. **30**, 2331 (2010)
27. L.W. Jiang, J. Zhou, X.Z. Yang, X.N. Peng, H. Jiang, D.Q. Zhuo, L.D. Chen, X.F. Yu, Chem. Phys. Lett. **510**, 135 (2011)
28. J. Zhang, Q.H. Chen, W.L. Zhang, S.L. Mei, L.J. He, J.T. Zhu, G.P. Chen, R.Q. Guo, Appl. Surf. Sci. **351**, 655 (2015)
29. J.Q. Zhuang, X.D. Zhang, G. Wang, D.M. Li, W.S. Yang, T.J. Li, J. Mater. Chem. **13**, 1853 (2003)
30. P.T. Shao, Q.H. Zhang, Y.G. Li, H.Z. Wang, J. Mater. Chem. **21**, 151 (2011)
31. J.S. Wang, H.E. Smith, G.J. Brown, Mater. Chem. Phys. **154**, 44 (2015)
32. M. Massey, M. Wu, E.M. Conroy, W.R. Algar, Curr. Opin. Biotech. **34**, 30 (2015)
33. Y. Kim, C. Ippen, T. Greco, I. Jang, S. Park, M.S. Oh, C.J. Han, J. Lee, A. Wedel, J. Kim, Electron. Mater. Lett. **10**, 479 (2014)
34. T.G. Kryshtab, L.V. Borkovska, O.F. Kolomys, N.O. Korsunska, V.V. Strelchuk, L.P. Germash, K.Y. Pechers'ka, G. Chornokur, S.S. Ostapenko, C.M. Phelan, O.L. Stroyuk, Superlattice. Microst. **51**, 353 (2012)
35. W.G. Becker, A.J. Bard, J. Phys. Chem. **87**, 4888 (1983)
36. B.A. Du, C. Liu, Y.H. Cao, L.N. Chen, Spectrosc. Spect. Anal. **34**, 1070 (2014)